**Supplementary information**

**Content**



## 1. Supplementary Methods

### *Clinical evaluation*

Medical history, physical examination and imaging were performed as part of routine clinical workup. For *MYL3* mutation-positive individuals, extensive clinical follow-up was performed (Table S1). The clinical evaluation was performed by experienced cardiologists. The conventional, two-dimensional and tissue doppler echocardiographic measurements of the heart of the individuals were evaluated by an echocardiologic examination. Neurophysiological studies were carried out in the proband (III.7) (Fig. 1A) from Family A by an experienced neurologist.

### *Genetic analysis*

*DNA isolation*

Blood samples were obtained from the patients, their parents, siblings and additional family members in some families. Extraction of genomic DNA was performed from whole blood,

using DNeasy Blood & Tissue kit (Qiagen, Hilden, Germany), according to the manufacturer's instructions.

*Next generation sequencing*

For **Family A**, exome sequencing was performed on DNA from the proband (III.7) and two clinically unaffected individuals in the family (III.1 and IV.3) (Fig. 1A), and data analysed through the use of the Ingenuity Variant Analysis (IVA) software (Qiagen, Hilden Germany), as previously described [1]. The filtering strategy focused on coding variants in known cardiac disease genes, selected based on variant databases Human Genome Mutation Database (HGMD) and ClinVar, and the most recent literature.

For **Family B**, exome sequencing was performed on DNA from the proband (IV.2) (Fig. 1B).

For **Family C**, exome sequencing was performed on DNA from the individual V.2, following the death of her daughter (VI.1), who was diagnosed with unclassified cardiomyopathy and died at the age of 8 of SCD (Fig. 1C). Variants were prioritized based on the following criteria: 1) The variant was predicted to perturb protein function. All synonymous and intronic variants were excluded unless the variant was within a predicted splice site (+ or -5 bp from splice junction). Any variation that was predicted to alter gene expression or protein function was included. These included nonsynonymous variations in coding regions (i.e. missense) or alterations resulting in frameshifts, premature stop codons, loss of stop codons, coding INDELS, and splice sites (i.e. ±2 nucleotides from an exon junction); 2) Homozygous variants; 3) The variant was rare as defined by allele frequency of less than 1% in either gnomAD or GME variomes; 4) The variant was present in a region of homozygosity as defined by HomozygosityMapper; 5) The variant was conserved evolutionarily as determined by a number of conservation scores including GERP (Score > 3), and PolyPhen2, SIFT, or predicted as disease causing by Mutation Taster for nonsense mutations.

Confirmatory bi-directional Sanger sequencing was performed in the probands in Families A and B and available family members from Families A, B and C (Fig. 1 and Fig. S2). PCR primers are available on request.

*Functional analysis of MYL3 in zebrafish*

All zebrafish studies were conducted in compliance with the UK Animals (Scientific Procedures) Act 1986. The studies were approved by a local (St George's University of London) ethical review committee and licensed under the Home Office granted project license P3DFD3131. Wildtype (AB × Tup LF) zebrafish were used for all zebrafish experiments. Antisense MO oligonucleotides (Genetools, LLC) were generated as previously described against the translational start site of cmlc1 (5'-TGGGTTCCACTTTTTTTGGTGCCAT-3') [2]. 100pg of Morpholino was injected into the yolk of 1–2 cell staged embryos and incubated at 28.5 °C until the desired stage. A control morpholino was used for comparison, targeting an intronic sequence in the human beta-globin gene. For *MYL3* rescue experiments, full human *MYL3* was commercially synthesized with *BamHI*/*XhoI* linkers, 5' and 3' respectively, and directionally cloned into pCS2+ at the *BamHI*/*XhoI* sites (GenScript). Patient variants were commercially generated using site directed mutagenesis of the pCS2+_*MYL3* construct (GenScript). DNA constructs were linearised using *NotI* restriction enzyme and RNA transcribed using the SP6 ambion MAXIscript kit, following the manufacturer's instructions. Approximately 100 pg of RNA was injected into the cytoplasm of wildtype one-cell staged embryos.

Fluorescent immunohistochemistry for MYH6 (supernatant S46, Developmental Studies Hybridoma Bank) and MYH1 (supernatant MF20, Developmental Studies Hybridoma Bank) were performed using standard techniques on 4% paraformaldehyde (PFA) fixed embryos and primary antibodies were diluted 1 in 5 for optimal results. Appropriate secondary

antibodies were used (ThermoFisher, cat # A21144 and A21121) at a 1 in 1000 dilution. Embryos were mounted on a 27mm glass bottom dish (ThermoFisher, cat # 150682) and imaged using a Nikon A1R confocal microscope.

The ventricular percentage shortening fraction was calculated from ventrally orientated videos of the heart (Supplementary Movies S9-13). Videos were converted to TIFF files using Adobe Photoshop CS6 and then imported as an image sequence into ImageJ for analysis. Average area measurements of diastolic and systolic ventricular state were taken over five cycles per embryos. The percentage shortening fraction was calculated as the percentage area change between diastolic and systolic state using the equation $100-\left[\frac{100}{\overline{x}\,\text{diastolic area}} \times \overline{x}\,\text{systolic area}\right]$. Statistical significance was evaluated using an unpaired t test in Graphpad Prism version 8.4.3.

*Minigene assay methods*

Minigene assays were performed as previously described [3, 4] with slight modifications. This assay relies on the use of a minigene vector which contains a fragment of the *SERPING1* gene, with two exonic regions separated by an intron, cloned into the mammalian expression vector pcDNA 3.1(-), downstream of the cytomegalovirus (CMV) promoter. Following transient transfection into human cells, chimeric transcripts can be analysed by reverse transcriptase PCR (RT-PCR) and sequencing. In brief, the exon of interest and 100-150 bp of flanking intronic sequence either side, were PCR amplified from patient and control DNA using 2X SuperFi (ThermoFisher Scientific) and cloned into the pCas2.1 minigene construct (a kind gift from Dr. Alexandra Martins) using *BamHI*/*MluI* (ThermoFisher Scientific) to generate pCas2.1-*MYL3*_e5 (https://benchling.com/s/seq-MpmgmQUFtsZtWsXCHHS9). The mutation of interest (c.482-1G>A) was incorporated using the Q5 site-directed mutagenesis kit (New England Biolabs). Mutagenesis oligos were as follows: *MYL3*_Q5SDM_FWD: 5'-ACTCCTGCCAaGTGAGAGGCT, and *MYL3*_Q5SDM_REV: 5'-GGGAGGCTGAGTCAGCAC. Plasmids were purified using a QIAprep miniprep kit

(QIAGEN) and sequences verified by Sanger sequencing. Expression constructs were then transfected into human HEK293FT cells using Lipofectamine 3000 (ThermoFisher Scientific), and RNA harvested after 24 hours using an RNeasy mini kit (QIAGEN). cDNA was generated using SuperScript III reverse transcriptase (ThermoFisher Scientific) and chimeric cDNA amplified by RT-PCR using 2X GoTaq G2 (Promega) using forward primer KO1F (5'-TGACGTCGCCGCCCATCAC) and reverse primer pCAS2R (5'-ATTGGTTGTTGAGTTGGTTGTC), with 30 cycles of amplification. RT-PCR products were analysed on a 2% agarose gel stained with ethidium bromide (0.5 μg/mL), and gel extracted and purified using a QIAquick gel extraction kit (QIAGEN) for Sanger sequencing. Splicing differences were assessed by comparing RT-PCR and sequencing results for the wild-type and variant (c.482-1G>A) constructs. Sequence alignments were performed in benchling (benchling.com) using the MAFFT algorithm. Two individual mutant clones were transfected and analysed to mitigate any potential issues (i.e. off-target effects) caused by site-directed mutagenesis.

## 2. Supplementary Results

*Cardiac and neurological evaluations of the patients*

**Case III.7** from Family A, is the second affected child of II.3 and II.4. The Echocardiogram evaluation indicated HCM Type III (Reverse Curvature type) with an ejection fraction (EF) of 55%, left atrium (LA) volume 52.2 mL and diameter 32 mm. Global Peak Systolic Strain (GLPS) was -24% and the ratio of the early mitral inflow velocity and mitral annular early diastolic velocity (E/e´) was 16.4 with a severe mitral regurgitation. Left ventricular outflow track (LVOT) gradient at rest and after maneuver was 9 and 30, respectively. Myocardial thickness was 19 mm at anteroseptal and 22 mm at lateral (Fig. S1). The Holter monitor test showed no arrhythmias. Her younger brother, III.8, was affected at an earlier age. Her mother (II.4) and her younger brother (III.8) died at the age of 55 and 26, respectively, of SCD. In

addition, her uncle (II.7) and her cousin (III.11) (Fig. 1A) died of SCD at the age of 57 and 24, respectively. There was, however, no record of cardiac evaluation available for these individuals. The echocardiography evaluation of individual III.6, who is from the same geographic region but not known to be related to the pedigree, indicated no signs of HCM (Table S1). The other apparently unaffected siblings and other family members showed no evidence of cardiac disease by history (Fig. 1A). The three asymptomatic children of the proband (IV.3, IV.4 and IV.5) 18, 13 and 6 years of age, respectively, were examined by a cardiologist and had normal echocardiograms at their current age (Table S1). The oldest daughter (IV.3) had, however, experiences of heart palpitations triggered by exercise. Follow-ups of all three children are warranted.

**Case IV.2,** from Family B, is the second child of asymptomatic first-cousin parents of Bakhtiyari ancestry. The Coronary CT angiography revealed chamber cardiomegaly. The patient had severe left ventricular (LV) dysfunction, with an LVEF of 15-20%, and moderate right ventricular (RV) dysfunction, defined as tricuspid annular plane systolic excursion (TAPSE)=9mm. ECG revealed rapid ventricular tachycardia. Clinical evaluation showed no evidence of cardiac disease in the 2 asymptomatic siblings (IV.3 and IV.4).

Given *MYL3* is also expressed in slow-twitch skeletal muscle fibers [5], a deleterious impact of *MYL3* variants on skeletal muscle function is possible. Therefore neurological evaluation was performed in the proband (Case III.7) from Family A. Affected individuals showed, however, no evidence of muscle weakness by neurological examination or by history. The neurological examination of the probands indicated no apparent muscle weakness. Muscle tone was normal and no distal or proximal muscle atrophy or fasciculation was detected in the limbs. The strength of muscle in the lower and upper limbs was 5/5. Levels of creatine phosphokinase were normal.

As in Family A, affected individuals from Family B showed no evidence of muscle weakness by history, suggesting that the recessive myosin ELC variant has little impact on skeletal muscle function.

*Genetic findings*

In Family A, the filtering strategy resulted in the identification of only one homozygous variant in a known cardiac disease gene, *MYL3* (c.170C>A (*rs*139794067), NM_000258.2) in individuals III:7 and IV:3. The variant converts a highly conserved amino acid alanine at position 57 to aspartic acid p.(Ala57Asp), which is located in the EF-hand $Ca^{2+}$ binding motif of ELC (Fig. 1D&E). The variant was identified in the heterozygous state in individual III.1. The *MYL3* variant was validated by PCR and bi-directional Sanger sequencing analysis in individuals III.1, III.7 and IV.3 (Fig. S2A). The presence of the *MYL3* variant was examined in all available family members by Sanger sequencing (Fig. S2A). Co-segregation studies confirmed that the apparently unaffected siblings and other family members were either heterozygous (III.1, III.4, III.6, IV.6 and IV.7) or wild-type (III.2, III.3, III.5 and IV.2) for the *MYL3* variant (Fig. 1A). Although individual III.6 is not known to be related to the pedigree, he is from the same region. All three asymptomatic children of the proband (IV.3, IV.4 and IV.5) were homozygous for this variant. There was, however, no DNA sample available for deceased family members II.4, II.7, III.8 and III.11.

In Family B, the filtering strategy resulted in the identification of only one homozygous variant in *MYL3* (c.106G>T), introducing a premature termination codon at position 36 p.(Glu36Ter) in individual IV.2. The *MYL3* variant was validated by PCR and bi-directional Sanger sequencing analysis in the parents III.1 and III.2, who were both carriers of the variant, and the two unaffected siblings IV.3 and IV.4, who were wild type and carriers, respectively (Fig. 1B and S2B).

Following the filtering strategy in Family C, the mother (V.2) of deceased individual (VI.1) (Fig. 1C), was found to harbor a heterozygous splice acceptor variant in *MYL3* (c.482-1G>A (*rs*727503300)). The variant was validated by PCR and bi-directional Sanger sequencing analysis, which confirmed the mother as a carrier and identified the father to also be a carrier. DNA from two of the mothers' siblings (V.3 and V.10) was available for testing, one of whom was wildtype (V.10) and the other (V.3) was found to be a carrier of the variant (Fig. 1C and S2C). Individual V.1 was also a carrier of the variant. Genetic testing of the two children VI.2 and VI.3 identified them as wild type and a carrier, respectively (Fig. 1C and S2C).

*Minigene assay of the MYL3* c.482-1G>A *variant*

The *MYL3* c.482-1G>A variant predominantly leads to skipping of the 78 bp exon 5 and a subsequent protein change p.(Gly161_Glu186del) (Fig. 2E-F). This would disrupt the last 3 AA of the EF-hand 2 domain, and the majority of the EF-hand 3 domain (Fig. 2I). The second (less frequent) consequence is a single nucleotide deletion of the first nucleotide of exon 5, as result of the G>A change generating a new splice acceptor site adjacent to the previous one (offset by 1nt). The first nucleotide of exon 5 (G) is instead considered intronic and is spliced out (Fig. 2G). As this is a single nucleotide deletion, it causes a frameshift leading to the p.(Gly161Valfs*4 protein change (as per HGVS guidelines) (Fig. 2G). This would completely abolish the EF-hand 3 domain and disrupt the last 3 (of 36) AA of the EF-hand 2 domain (Fig. 2I).

Based on quantitation by densitometry, the exon skipping event is more frequent (around 75%) compared to the single nucleotide deletion (~25%) (Fig. 2F), presumably as the latter uses 'less preferred' nucleotides either side of the consensus splice nucleotides (AG). However, it should be noted that the RT-PCRs are only semi-quantitative, and the minigene assays may not completely recapitulate *in vivo* splice event frequencies.

**Web resources**

The following databases were used in this study:

The Exome Variant Server: NHLBI Exome Sequencing Project (ESP), Seattle, WA;

URL: http://evs.gs.washington.edu/EVS/

1000 Genome Project Database: http://browser.1000genomes.org/index.html

Human Background Variant DataBase: http://neotek.scilifelab.se/hbvdb/

Genome Aggregation Database (GnomAD): http://gnomad.broadinstitute.org/

ClinVar: http://www.ncbi.nlm.nih.gov/clinvar/

Human Gene Mutation Database: http://www.hgmd.cf.ac.uk/ac/index.php

Greater Middle East (GME) Variome web: http://igm.ucsd.edu/gme/index.php

Ensembl genome browser: http://www.ensembl.org/

MutationTaster: http://mutationtaster.org/

PMut: http://mmb.irbbarcelona.org/PMut

PolyPhen-2: http://genetics.bwh.harvard.edu/pph2/

SIFT: http://sift.bii.a-star.edu.sg/

Uniprot: https://www.uniprot.org/uniprot/P08590

## 3. Supplementary Tables

**Table S1:** Clinical findings of family members in Families A and B

| Family ID | Individual | Age at examination (year) | Sex | Echocardiographic Findings | | | | | |
|---|---|---|---|---|---|---|---|---|---|
| | | | | ST (mm) | PWT (mm) | Maximum wall thickness (mm) | LVEDD (mm) | LVESD (mm) | LVEF (%) |
| A | III.6 | 45 | M | 8 | 8 | NC | 49 | 30 | 60 |
| A | III.7 | 38 | F | 11 | 9 | 22 (Anterolateral) | 40 | 22 | 55 |
| A | IV.3 | 18 | F | 7 | 7 | 7 | 42 | 26 | 60 |
| A | IV.4 | 13 | F | 7.2 | 6.8 | 7.2 | 38 | 25 | 60 |
| A | IV.5 | 6 | M | 6 | 6.3 | 6.3 | 31 | 25 | 60 |
| B | IV.2 | 6 | M | 7.1 (IVSd) 7.8 (IVSs) | 5.8 (LVPWd) 5.2 (LVPWs) | NC | 50.6 (LVIDd) | 45.4 (LVIDs) | 22 |

Abbreviations: F: Female; M: Male; ST: Septal thickness; PWT: Posterior wall thickness; LVEDD: Left ventricular end-diastolic diameter; LVESD: Left ventricular end-systolic diameter; LVEF: Left ventricular ejection fraction; IVSd: Interventricular septum thickness end-diastolic diameter; IVSs: Interventricular septum thickness end-systole diameter; LVPWd: Left ventricular posterior wall end-diastolic diameter; LVPWs: Left ventricular posterior wall end-diastolic diameter; LVIDd: Left ventricular internal end-diastolic diameter; LVIDs: Left ventricular internal end-systolic diameter; NC: not conducted.

**Table S2:** Variant details including genomic and cDNA annotations, predicted protein changes, variant allele frequencies from across a number of databases and scoring based on ACMG criteria (Richards *et al.*, 2015). VUS, variant of uncertain significance.

| **Variant annotation** | Genomic position, GRCh38/hg38 (DNA change) | chr 3:46860813 (C>A) | chr 3:46863285 (G>T) | chr 3:46858462 (G>A) |
|---|---|---|---|---|

| | | | | |
|---|---|---|---|---|
| | Transcript change (NM_000258.2) | c.170C>A | c.106G>T | NC_000003.12: c.482-1G>A |
| | Protein change (NP_000249.1) | p.(A57D) | p.(E36*) | p.Gly161_Glu186del & p.Gly161Valfs*4 |
| | dbSNP ID | *rs*139794067 | - | rs727503300 |
| | Variant seen in family | A | B | C |
| | Size of the region of homozygosity | Chr 3: 45187785-52537648 and 52676066-54401650 | Chr 3: 41288466-53891594 (12.6Mb) | NA |
| **Allele frequencies (PM2)** | gnomAD (no. homozygous) | 0.000163 (0) | Absent | Absent |
| | NHLBI Exome Sequencing Project. (no. homozygous) | 0.0004539 (0) | Absent | Absent |
| | In-House Databases, QSG/ ((no. homozygous) | 21/16000 (0) | Absent | Absent |
| | Iranome | Absent | Absent | Absent |
| | GME Variome (no. homozygous) | 0.001007 (0) | Absent | Absent |
| ***In silico* predictions (PP3)** | CADD | 28.200 | 35 | - |
| | GERP | 2.45 | - | - |
| | Polyphen | Probably damaging | - | - |
| | SIFT | Damaging | - | - |
| | MutationTaster | Disease causing | Disease causing | Disease causing |
| **Additional ACMG** | Support from cosegregation | Yes (homozygous in the proband and | Yes (homozygous in the proband and | Yes, parents and unaffected siblings from 2 branches of the |

| | | | | |
|---|---|---|---|---|
| **criteria and classification** | within family (PP1) | heterozygous in unaffected individuals) | heterozygous in unaffected individuals) | extended family are heterozygous or homozygous for wildtype |
| | ClinVar | Conflicting interpretations of pathogenicity | Absent | Absent |
| | Null variant (nonsense, frameshift, canonical splice site) (PVS1) | No | Yes (moderate) | No |
| | Functional studies supportive of a damaging effect on the gene (PS3) | Yes | Yes | No |
| | Parental testing supportive of occurrence of variants in *trans* (PM3) | Yes | Yes | Yes |
| | Protein length changes due to in-frame deletions/insertions and stop losses (PM4) | No | Yes | Yes |
| | Overall classification | VUS (PM2, PP3, PP1, PM3, PS3) | Pathogenic<br><br>(PM2, PP3, PP1, PVS1_Moderate, PM3, PM4, PS3) | Likely pathogenic (PM2, PP3, PP1, PM3, PM4, PS4) |

## 4. Supplementary References


1. Kariminejad A, Dahl-Halvarsson M, Ravenscroft G, et al. TOR1A variants cause a severe arthrogryposis with developmental delay, strabismus and tremor. *Brain.* 2017; **140**: 2851-9.
2. Chen Z, Huang W, Dahme T, et al. Depletion of zebrafish essential and regulatory myosin light chains reduces cardiac function through distinct mechanisms. *Cardiovasc Res.* 2008; **79**: 97-108.
3. Gaildrat P, Killian A, Martins A, et al. Use of splicing reporter minigene assay to evaluate the effect on splicing of unclassified genetic variants. *Methods Mol Biol.* 2010; **653**: 249-57.

4. Gaildrat P, Krieger S, Di Giacomo D, et al. Multiple sequence variants of BRCA2 exon 7 alter splicing regulation. *J Med Genet.* 2012; **49**: 609-17.
5. Morano I. Tuning the human heart molecular motors by myosin light chains. *J Mol Med (Berl).* 1999; **77**: 544-55.

## 5. Supplementary Figures

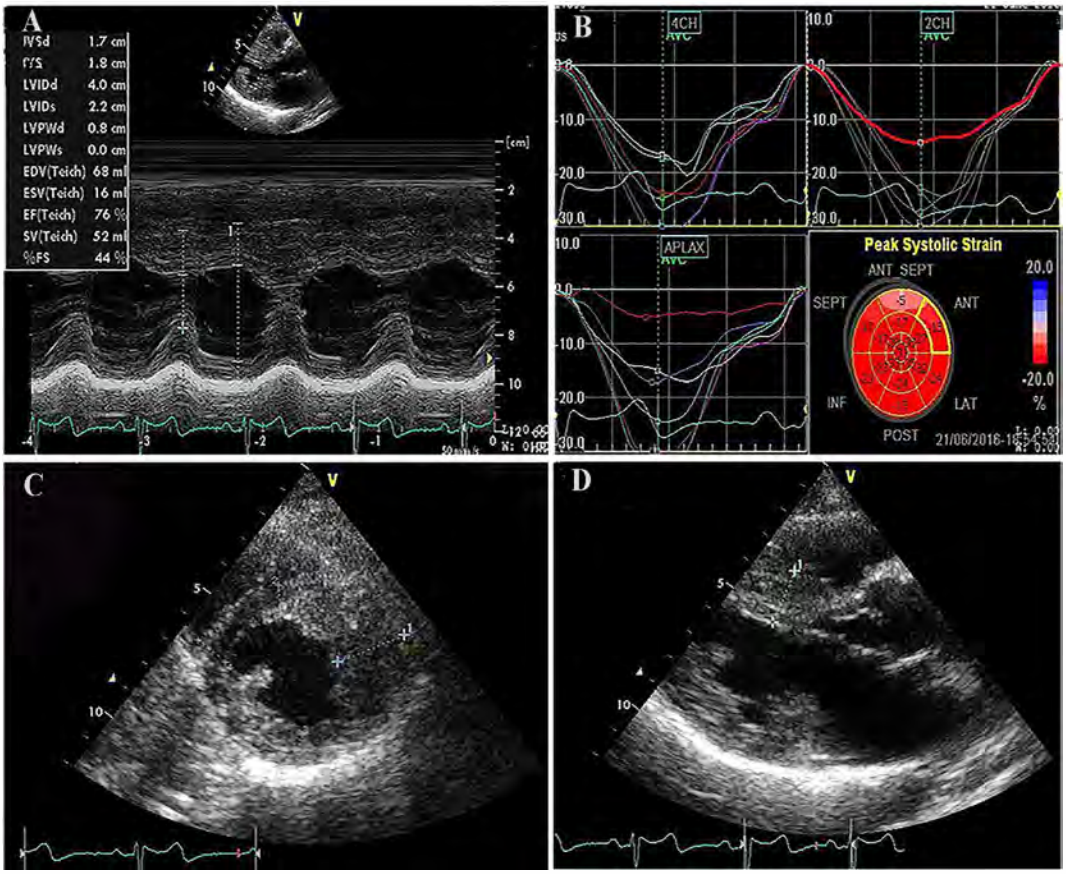
A
IVSd 1.7 cm
IVSs 1.8 cm
LVIDd 4.0 cm
LVIDs 2.2 cm
LVPWd 0.8 cm
LVPWs 0.0 cm
EDV(Teich) 68 ml
ESV(Teich) 16 ml
EF(Teich) 76 %
SV(Teich) 52 ml
%FS 44 %
[cm]
B
4CH
2CH
APLAX
Peak Systolic Strain
ANT SEPT
SEPT
ANT
INF
LAT
POST
20.0
-20.0
%
C
D

**Supplementary Figure 1: Clinical images of the proband (III.7) from Family A**

(**A**) M-Mode measurement of LV size and wall thickness. (**B**) 2D strain of LV, and Global Peak Systolic Strain (GLPS) reveals reduced strain at the same segment of significant hypertrophy. (**C**) 2D echocardiography at short axis view reveals asymmetric hypertrophy of anterior, anterolateral and lateral segments of LV, (**D**) compatible with anteroseptal hypertrophy and sparing posterior wall as asymmetric LVH in 2D echocardiography.

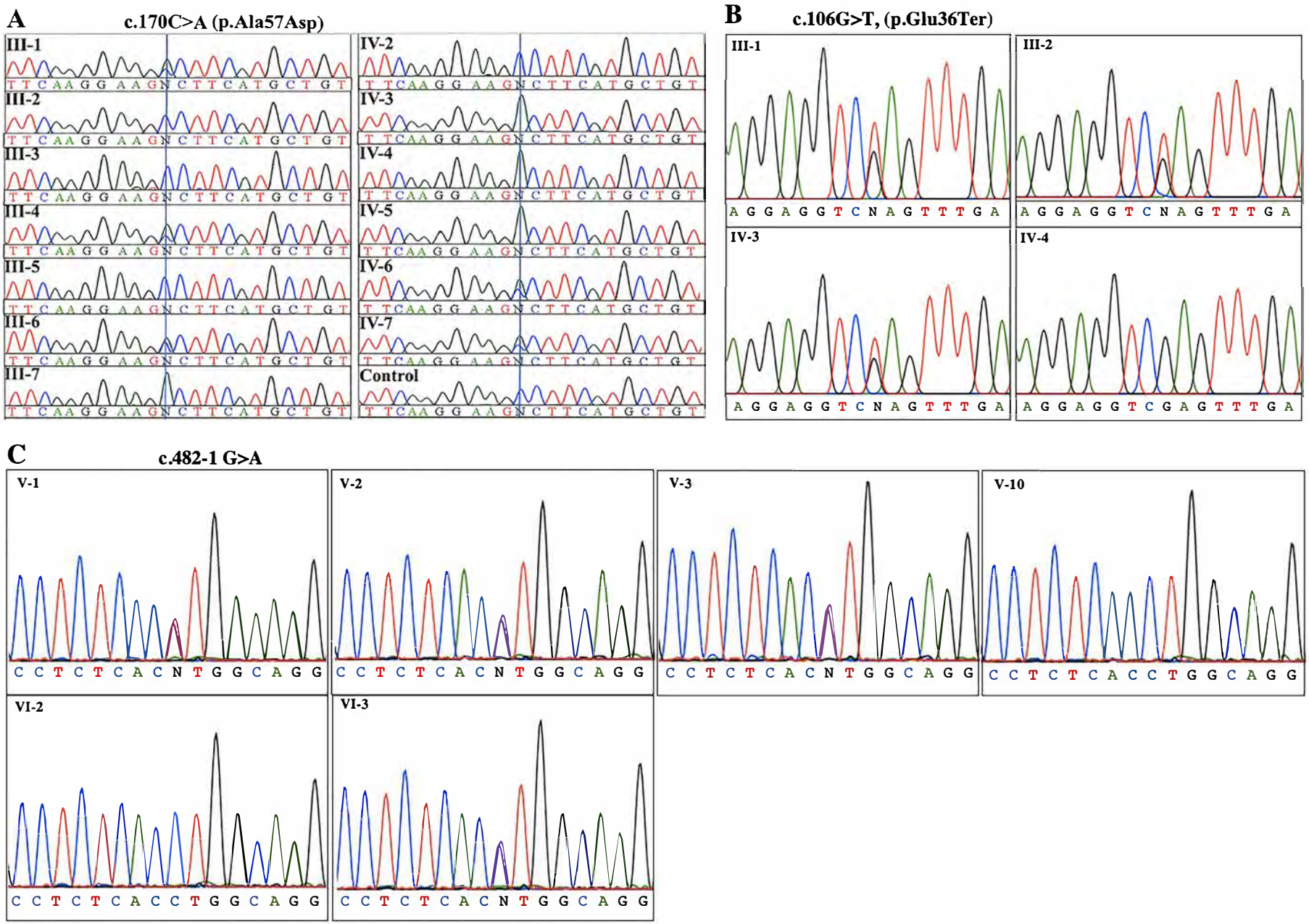
A
c.170C>A (p.Ala57Asp)
III-1
III-2
III-3
III-4
III-5
III-6
III-7
IV-2
IV-3
IV-4
IV-5
IV-6
IV-7
Control
B
c.106G>T, (p.Glu36Ter)
III-1
III-2
IV-3
IV-4
C
c.482-1 G>A
V-1
V-2
V-3
V-10
VI-2
VI-3

**Supplementary Figure 2. Genetic findings**

(**A**) Sanger sequence analysis demonstrates the presence of homozygous *MYL3* c.170C>A, p.(Ala57Asp) variant in the proband and her three children, and the segregation of the variant. (**B**) Sanger sequence analysis demonstrates the presence of heterozygous *MYL3* c.106G>T, p.(Glu36Ter) variant in the probands parents, and one sibling (IV.4), the other sibling (IV.3) is wild type. (**C**) Sanger sequence analysis demonstrates heterozygosity for the *MYL3* c.482-1 G>A variant in the proband's parents, and one sibling (VI.3), the other sibling (VI.2) is wild type. Sanger traces are also available for two siblings of the mother, one of whom (V.3) is heterozygous, and the other (V.10) is wild-type.

## 6. Supplementary Movie legends

Movie (**S1)** Sham (H2O) injected control embryos at 48 hpf show normal blood flow and heart function. Movie (**S2**) Embryos injected with a *cmlc1* targeted morpholino develop obstructed blood flow due to perturbed ventricular contractions. Blood can be seen in the contracting dilated atrium but fails to propagate through the non-functioning ventricle at 48 hpf. Movie (**S3**) Embryos injected with *MYL3* RNA alone develop normal functioning hearts. Movie (**S4**) At 48 hpf, embryos injected with both cmlc1MO and *MYL3* RNA maintain ventricular function and cardiac blood flow. Indicating that injections of wildtype *MYL3* RNA can rescue the cmlc1 morphant phenotype. Movie (**S5**) Embryos injected with *MYL3* RNA containing the c.170C>T (p.(Ala57Asp)) variant develop normal functioning hearts. Movie (**S6**) At 48 hpf, embryos injected with both *cmlc1*MO and the c.170C>T *MYL3* RNA display partial rescue of heart morphology and function, indicated by observed atrial edemas, some regurgitation but improved blood flow. Movie (**S7**) At 48 hpf, embryos injected with both *cmlc1*MO and the c.106G>T *MYL3* RNA display heart edemas, dysfunctional ventricles and dilated atriums common to *cmlc1* morphants. Indicating that injections of c.106G>T *MYL3* is not sufficient to rescue the cmlc1 morphant phenotype. Movie (**S8**) Embryos injected with *MYL3* RNA containing the c.106G>T (p.(Glu36Ter)) variant develop normal functioning hearts. **S9-13** show representative examples of ventrally orientated con (**S9**), cmlc1 MO (**S10**), cmlc1 MO + *MYL3* RNA (**S11**), cmlc1 MO + c170C>T *MYL3* RNA (**S12**), and cmlc1MO + c.106G>T *MYL3* RNA (**S13**) embryos at 48 hpf.